

To study expression and assembly of TRPM1 channels we cloned seven full lengths TRPM1 cDNAs from mouse eye which represent splice variants and encode proteins of 1462, 1506, 1512, 1578, 1584, 1622 and 1628 amino acid residues. These TRPM1 protein variants vary in their N terminus, in a putative extracellular loop and the predicted pore region. For expression analyses we prepared polyclonal and monoclonal antibodies directed against various antigenic epitopes of TRPM1. All antibodies detect proteins of the size expected for TRPM1 in the eye, in lung and skeletal muscle. They immunoprecipitate the TRPM1 protein from mouse retina and specifically label postsynaptic dendrites of bipolar cells adjacent to the ribbon synapse. All TRPM1 proteins contain a coiled-coil domain in their C termini and isolated fragments comprising this coiled-coil domain have been shown to form dimers (1). We show that after disruption of this coiled-coil domain by site directed mutagenesis the full-length TRPM1 proteins still assemble to dimers and higher molecular protein complexes and interact with each other, apparently by additional intermolecular interactions of TRPM1 sequences within the N-terminus. Similarly, a related TRPM protein, TRPM4, still forms dimers after destruction of a C-terminal coiled-coil domain, most probably via interactions of N-terminal protein sequences.

1 Tsuruda PR, Julius D, Minor DL Jr (2007) *Neuron* 51, 201-212.

1789-Pos

A Reduction of Glucose-Induced Bursting Frequency in Pancreatic Islets Correlates with Decreased Insulin Release and Impaired Glucose Tolerance in TRPM5^{-/-} Mice

Barbara Colasoul¹, Anica Schraenen¹, Katleen Lemaire¹, Roel Quintens¹, Leentje Van Lommel¹, Andrei Segal¹, Robert Margolske², Zaza Kokrashvili², Grzegorz Owsianick¹, Karel Talavera¹, Thomas Voets¹, Patrick Gilon³, Bernd Nilius¹, Frans Schuit¹, Rudi Vennekens¹.

¹K.U.Leuven, Leuven, Belgium, ²Mount Sinai School of Medicine, New York, NY, USA, ³Universite Catholique de Louvain, Bruxelles, Belgium. Glucose homeostasis is critically dependent on insulin release from pancreatic beta cells, which is strictly regulated by glucose-induced simultaneously oscillations in membrane potential (V_m) and cytosolic calcium concentrations $[Ca^{2+}]_{cyt}$. We propose that TRPM5, a Ca^{2+} -activated monovalent cation channel, is a positive regulator of glucose-induced insulin release. Micro-array screening and immunostaining reveal high and selective expression of TRPM5 in pancreatic islets. Whole cell current measurements in WT pancreatic islet cells demonstrate a Ca^{2+} -activated non-selective cation current with properties comparable to TRPM5 measured in over-expression, including the bell-shaped dependency on intracellular Ca^{2+} , time constant of activation and permeation properties. This current is significantly reduced in *Trpm5*^{-/-} cells. Ca^{2+} -imaging and electrophysiological analysis show that glucose-induced oscillations of V_m and $[Ca^{2+}]_{cyt}$ have a reduced frequency in *Trpm5*^{-/-} islets. WT islets display either slow or fast oscillations, or mixed oscillations, consisting of fast oscillations superimposed on slow ones. In contrast, *Trpm5*^{-/-} islets never show a fast oscillation pattern. Fast oscillations in V_m show a shorter burst interval, due to a higher slope of depolarization towards the threshold potential for burst initiation. Our results indicate that TRPM5 accelerates the depolarization during the interburst interval, initiating rapid oscillations and higher insulin release. As a consequence, glucose-induced insulin release from *Trpm5*^{-/-} pancreatic islets is significantly reduced, resulting in an impaired glucose tolerance in these mice. Pharmacological modulation of TRPM5 activity may represent a novel means to adjust insulin release in diabetic patients.

1790-Pos

Physiological Role of the Oxidative Stress-Sensitive TRPM2 Ca^{2+} Channel in Immunocytes

Shinichiro Yamamoto, Hiroshi Takeshima, Yasuo Mori.
Kyoto University, Kyoto, Japan.

It is known that a large amount of reactive oxygen species (ROS) exist at inflamed sites. ROS induce chemokines responsible for the recruitment of inflammatory cells at inflamed sites. Here, we demonstrate that the plasma membrane Ca^{2+} -permeable channel TRPM2 controls ROS-induced chemokine production in monocytes/macrophages. In monocytes from *Trpm2*-deficient mice, H_2O_2 -induced Ca^{2+} influx and production of the macrophage inflammatory protein-2 (CXCL2), which exhibit potent neutrophil chemotactic activity, were impaired. In the inflammation model dextran sulfate sodium-induced colitis, CXCL2 expression was attenuated by *Trpm2* disruption. Interestingly, the number of recruited neutrophils was significantly reduced in DSS-treated *TRPM2* KO mice, whereas that of DSS-induced macrophages after infiltration into inflamed sites, was indistinguishable in WT and *TRPM2* KO mice. Importantly, *TRPM2* deficiency failed to impair important aspects of CXCL2-evoked neutrophil chemotaxis, including Ca^{2+} response, *in vitro* migration, and *in vivo* infiltration after DSS administration. Thus, TRPM2-mediated Ca^{2+} influx

induces chemokine production in monocytes that aggravates inflammatory neutrophil infiltration. We propose functional inhibition of TRPM2 channels as a new therapeutic strategy for treating inflammatory diseases.

1791-Pos

Multi-Dimensional Characterization of the Desensitization Behavior of Temperature- and H⁺-Activated Human TRPV1 Channels using Microfluidics

Maria Millingen, Erik T. Jansson, Per Lincoln, Aldo Jesorka, Owe Orwar.
Chemical and Biological Engineering, Göteborg, Sweden.

This work describes the pH- and temperature-dependence of acute desensitization and tachyphylaxis in human TRPV1 channels. We use an in-house developed microfluidic device and associated methods, which independently can control the temperature and the solution environment (e.g. the pH) around patch-clamped cells, as well as the time a cell is exposed to different solutions. Thus, cells can be stimulated and controlled in a multi-dimensional parameter space. Our results show that if TRPV1 channels are exposed repeatedly to low pH applications, the rate of desensitization becomes progressively slower, whereas the rate of channel activation remains unchanged. Also, both the rate of activation and the rate of acute desensitization increase at higher temperatures. The extent of tachyphylaxis is found to be dependent on pH, temperature, and exposure time. We also show that both the desensitization rate and the extent of tachyphylaxis are correlated to current density. This could be due to the fact that Ca^{2+} is an important factor for both acute desensitization and tachyphylaxis, and since TRPV1 is permeable to Ca^{2+} , the current density is proportional to Ca^{2+} influx.

1792-Pos

A Novel Tarantula Toxin Irreversibly Activates TRPV1

Christopher J. Bohlen¹, Avi Priel¹, Jan Siemens^{1,2}, David Julius¹.

¹University of California, San Francisco, San Francisco, CA, USA,

²Max-Delbrück-Centrum für Molekulare Medizin, Berlin, Germany.

Spider venoms contain an evolutionarily honed pharmacopeia of natural toxins that target membrane receptors and ion channels to produce shock, paralysis, pain, or death. Toxins evolve to interact with functionally important protein domains, including agonist binding sites, ion permeation pores, and voltage-sensing domains, making them invaluable reagents with which to probe mechanisms underlying channel activation or modulation. We have identified a novel tarantula peptide toxin that serves as an irreversible agonist for the heat/capsaicin-activated channel, TRPV1. The toxin contains two independently functional Inhibitor Cysteine Knot (ICK) domains, endowing it with an antibody-like bivalency that results in extremely high avidity for its multi-meric channel target. We are using this new toxin as a tool to help dissect the unique properties of TRPV1.

Muscle: Fiber & Molecular Mechanics & Structure II

1793-Pos

Passive Force Augmentation in Actively Stretched Myofibrils and Sarcomeres

Tim R. Leonard, Walter Herzog.

University of Calgary, Calgary, AB, Canada.

Single skeletal muscle myofibrils were stretched actively and passively ($pCa^{2+} = 3.5$ and 8 respectively) from optimal length to beyond myofilament overlap (4.0 μm) and individual sarcomere lengths and the associated stretch forces were measured. Actively stretched myofibrils produced much more force than passively stretched myofibrils at all sarcomere lengths, including when all sarcomeres were beyond myofilament overlap (Figure 1). In order to confirm that cross bridge based acto-myosin forces were not present at sarcomere lengths beyond myofilament overlap, passively and actively stretched myofibrils were deactivated and activated, respectively at 5 μm . In both cases,

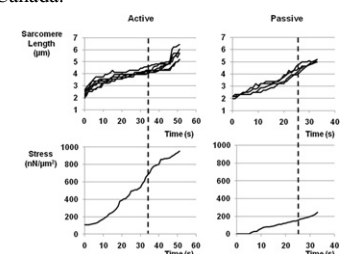


Figure 1. Individual sarcomere length and force traces for single active and passive myofibrils. Actively stretched myofibrils show much greater force than passively stretched myofibrils at sarcomere lengths beyond myofilament overlap where actin-myosin based cross-bridge forces are zero. Dashed vertical line denotes when all sarcomeres are beyond myofilament overlap.

no change in force was observed, indicating that active cross bridge forces were not present at long (5 μ m) length. Based on these results, we suggest that there is a dramatic passive force augmentation in passively stretched myofibrils and the individual sarcomeres.

1794-Pos

Role of Sarcomere Disruption in Stretch-Induced Force Loss of Myofibrils Appaji Panchangam, Walter Herzog.

University of Calgary, Calgary, AB, Canada.

Stretching of activated skeletal muscle results in loss of force. In the absence of direct evidence, it is often assumed that sarcomere disruption is the cause of stretch-induced force loss. We stretched mechanically isolated rabbits psoas myofibrils on the descending limb of the length-tension relationship and asked the specific questions: does sarcomere disruption occur and does it affect the magnitude of stretch-induced force loss? Myofibrils were mounted on an inverted microscope with one end attached to a glass micro needle and the other to a silicon nitrate force lever. Myofibrils (n=11) were maximally activated at an average resting sarcomere length of $2.8 \pm 0.2 \mu\text{m}$. At peak isometric stress ($234 \pm 92 \text{ kN m}^{-2}$), myofibrils were stretched by $34.3 \pm 5.2 \%$ at a speed of 3.3 s^{-1} and immediately returned to the reference lengths at the same speed. Myofibrils were subsequently relaxed and re-activated after 3-5 minutes of rest to reassess post-stretch stress. Post-stretch isometric stress was reduced by $34 \pm 9.6 \%$ compared with pre-stretch stress. Eight out of 11 myofibrils had no sarcomere disruption after stretching while the remaining 3 myofibrils had a small percentage of sarcomeres pulled beyond filament overlap suggesting sarcomere disruption. The average stress reduction in the disrupted and non-disrupted myofibrils was the same ($27 \pm 13 \%$ vs $36 \pm 8\%$; $p = 0.83$). We conclude from these results that stretch-induced loss of force in myofibrils can occur in the absence of sarcomere disruption, and that sarcomere disruption does not increase force loss following myofibril stretch.

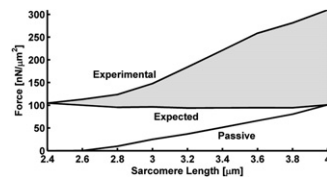
1795-Pos

Active Force Augmentation for Physiologically Relevant Stretches in Myofibrils and Mechanically Isolated Sarcomeres

Azim Jinha, Tim R. Leonard, Walter Herzog.

University of Calgary, Calgary, AB, Canada.

We reported previously that forces in actively stretched myofibrils and sarcomeres were up to four times greater than forces in passively stretched myofibrils at sarcomere lengths $>4 \mu\text{m}$. These increased forces were independent of actin-myosin based cross-bridge forces and were absent when titin was eliminated. Here, we demonstrate that such force augmentation also occurs for physiologically relevant sarcomere lengths (2.4-4.0 μm). Actin-myosin based cross-bridge forces and non cross-bridge based forces were distinguished by assuming that sarcomeres reached a steady-state cross-bridge distribution in the first 0.4 μm of stretch. The forces due to stretching could then be calculated and added to the passive forces measured during passive stretching (Figure 1) to obtain the expected forces during active stretching. Subtracting the expected from the experimentally measured forces during active stretching, the force augmentation was obtained. Mean force augmentation towards the end stretching reached values in excess of the mean maximal active isometric forces at optimal sarcomere length, suggesting that force augmentation not associated with actin-myosin based cross-bridge forces is highly relevant in actively stretched myofibrils and isolated sarcomeres.



1796-Pos

The Contribution of Calcium and Stretch-Activated Tension to Power Generation by *Drosophila* Indirect Flight Muscle

Qian Wang, Cuiping Zhao, Douglas M. Swank.

Rensselaer Polytechnic Institute, Troy, NY, USA.

Recent studies suggest small insects might regulate muscle power output by operating their stretch activated indirect flight muscles (IFM) at less than saturating calcium levels during flight instead of varying the number of muscle fibers recruited. Calcium levels have also been found to correlate with wing beat frequency, suggesting calcium concentration might influence aerodynamic power. To test the effects of calcium concentration on muscle power generation, we used the work loop technique to measure *Drosophila* indirect flight muscle (IFM) oscillatory power generation under optimal length change parameters. Maximum power was $2.2 \pm 0.4 \text{ nW/mm}^3$ at $p\text{Ca} = 4.7 \pm 0.09$. The threshold for muscle power generation occurs at $\sim p\text{Ca} 6.1$, with $p\text{Ca}_{50} = 5.8 \pm 0.05$ and the Hill coefficient = 7.2 ± 3.7 . Over the steepest portion of the curve, and above the estimated minimum power required for flight, about $p\text{Ca} 6.0$

to 5.5, muscle power increases 2.5-fold. We compared the contributions to muscle power from calcium activated isometric tension to the contribution from the tension generated by stretch-activation during flight by imposing a 2.5% ML, 1.5 ms stretch. The $p\text{Ca}_{50}$ for calcium activated tension was 6.1 ± 0.05 and Hill coefficient was 4.6 ± 1.3 . The $p\text{Ca}_{50}$ for stretch activated tension was 5.8 ± 0.07 and Hill coefficient was 3.8 ± 1.3 . Following a stretch at $p\text{Ca} 4.5$, total isometric tension increased from $2.5 \pm 0.3 \text{ mN/mm}^2$ to $16.4 \pm 1.2 \text{ mN/mm}^2$ of which $11.4 \pm 1.1 \text{ mN/mm}^2$ was contributed by passive elastic elements. As calcium is increased from $p\text{Ca} 6.0$ to 5.5, stretch-activated tension contributes $1.0 \pm 0.3 \text{ mN/mm}^2$ of additional tension while calcium tension contributes $0.4 \pm 0.2 \text{ mN/mm}^2$. We conclude that if calcium levels vary between $p\text{Ca} 6.0$ to 5.5 during flight, then the contribution of stretch tension to additional power is about twice that of calcium tension.

1797-Pos

Dual Regulation Mechanisms for Ca^{2+} -Activated and Stretch-Activated Forces in Asynchronous Flight Muscle of Insect: Mechanical and X-Ray Evidence

Hiroyuki Iwamoto.

Spring-8, JASRI, Sayo-gun, Hyogo, Japan.

During flight of insects, their flight muscles (IFMs) are often endothermically maintained at an optimal temperature. In the case of bumblebee, this temperature is $\sim 42^\circ\text{C}$. At saturating $[\text{Ca}^{2+}]$, glycerinated bumblebee IFM fibers develop large Ca^{2+} -activated (CA) force of $\sim 50 \text{ kPa}$ above 20°C , as well as stretch-activated (SA) force. Below the critical temperature of 15°C , the CA force is sharply suppressed. Surprisingly, the SA force is not suppressed even at 5°C . This suggests that the inhibition of CA force at low temperatures is not due to myosin inactivation, but it is an issue of regulation. The CA force- $p\text{Ca}$ curve remains sigmoidal at lower temperatures, and the $p\text{Ca}_{50}$ value is only slightly affected, indicating that myosin is unable to develop large CA force even if troponin is saturated with Ca^{2+} . The mechanism for temperature-dependent CA force regulation is further investigated by X-ray diffraction, by recording semi-static patterns in the stretch and release phases of a repeated stretch-release protocol. At 5°C , the 2nd actin layer line (ALL) is increased from 5% at rest (relative to 6th ALL) to 19% in the release phase, indicating that the myosin binding sites on actin are almost fully open even when the CA force is suppressed. In the stretch phase, the 2nd ALL is further enhanced to 26%. At 20°C , the 2nd ALL intensity is enhanced to 25 and 29% in the release and stretch phases, respectively. These results suggest that a pathway after thin-filament activation is blocked at low temperatures, and SA force could be regulated independently of this pathway. The critical temperature for CA force development is also found in other insects, such as a true bug *Nezara* ($T=20\text{-}25^\circ\text{C}$), but not in a giant waterbug *Lethocerus*.

1798-Pos

Contractile Properties of Human Fetal Skeletal Muscle Proteins

Alice W. Ward, Galina Flint, Anita E. Beck, Michael J. Bamshad, Michael Regnier.

University of Washington, Seattle, WA, USA.

Congenital contracture syndromes associated with myofilament proteins are present in 1 out of every 1000 live births. Because the myosin heavy chain protein family has several isoforms unique to the pre-natal development of muscle, it is important to know the contractile properties of this tissue to determine how mutations affect performance and development. However, information on human fetal muscle contractile properties is lacking. We are beginning to characterize the contractile properties of this tissue using in vitro motility assays, where we can deconstruct which proteins of developing muscle can be attributed to differences seen in patients with congenital contracture syndromes. Embryonic myosin was isolated from human fetal muscle samples at 15.4 weeks gestation. An in vitro motility assay was performed at 30 degrees C with an ionic strength of 0.17 to determine the predominant myosin's enzymatic properties. The max speed of filaments on human fetal skeletal myosin (1.9 $\mu\text{m/s}$) was significantly lower than filaments on adult rat skeletal myosin (4.8 $\mu\text{m/s}$) under the same conditions. The K_m values were similar between the human fetal (0.02 mM) and adult rat (0.03mM) myosins. Ongoing work includes studying the effects of increased ADP, substitution of ATP with dATP, studying Ca^{2+} regulation of in vitro motility assays using actin and thin filament regulatory proteins purified from fetal muscle of approximately the same gestational period, and skinned muscle cell experiments. By utilizing these assays, we can develop a more mature understanding of muscle contraction during development and form better hypotheses about the mechanism of how specific mutations lead to these contracture syndromes. Establishing these contractile properties will lead to better hypotheses regarding the development of contractures in utero and how it is affected by mutations associated with congenital contracture syndromes. Supported by HL65497 (Regnier) and HD48895 (Bamshad).